BMC Ophthalmology

RESEARCH

Open Access

Peripapillary Bruch's membrane Opening-Minimum Rim Width (BMO-MRW) and microvascular changes in early diabetic retinopathy

Jun Zhou[1†], Xiangning Wang[1†], Wei Lou[1†], Tingting Li[1], Ye Zhang[1], Ying Hu[1], Da Long[1], Xueyan Zhang[1*] and Qiang Wu[1*]

Abstract

Background To evaluate changes in peripapillary Bruch's Membrane Opening-Minimum Rim Width (BMO-MRW) and its association with peripapillary microvascular in patients with early diabetic retinopathy (DR).

Methods This observational cross-sectional study included 105 eyes from 105 diabetic patients, comprising 55 eyes without diabetic retinopathy (No-DR group) and 50 eyes with mild diabetic retinopathy (Mild-DR group). An additional 50 eyes from 50 healthy individuals served as the Control group. All eyes underwent optical coherence tomography (OCT) radial scanning to assess Bruch's membrane opening-minimum rim width (BMO-MRW) and OCT-angiography (OCTA) with a 6 mm × 6 mm scan centered on the optic disc to evaluate perfusion density (PD) and vessel density (VD). OCTA measurements were calibrated based on the FoBMO axis and analyzed using the ETDRS grid. The associations between BMO-MRW and PD/VD were subsequently investigated.

Results The mean BMO-MRW values were significantly lower in the No-DR (305.78 ± 35.12 μm) and Mild-DR groups (299.42 ± 37.33 μm) compared to the control group (323.56 ± 40.33 μm, $P = 0.005$), with significant thinning in the superotemporal and inferotemporal quadrants ($P = 0.039$, 0.047). PD in the inner ETDRS grid decreased from (56.01 ± 10.53)% in the control group to (52.16 ± 8.75)% in the No-DR group and (47.91 ± 12.95)% in the Mild-DR group ($P = 0.001$), while in the outer ETDRS grid, it declined from (42.92 ± 6.70)% to (40.20 ± 7.24)% and (38.13 ± 8.78)%, respectively ($P = 0.008$). VD in the inner ETDRS grid showed a reduction from (15.41 ± 2.68) mm^{-1} in the control group to (14.39 ± 2.17) mm^{-1} in the No-DR group and (13.55 ± 2.98) mm^{-1} in the Mild-DR group ($P = 0.001$), while in the outer ETDRS grid, it decreased from (13.74 ± 2.26)mm^{-1} to (12.78 ± 2.53)mm^{-1} and (12.09 ± 2.83)mm^{-1}, respectively ($P = 0.006$). Significant reductions in PD were observed in the nasal quadrant of the inner ring and the supratemporal quadrant of

[†]Jun Zhou, Xiangning Wang and Wei Lou contributed equally to this work.

*Correspondence:
Xueyan Zhang
zhangxueyan175@163.com
Qiang Wu
qiang.wu@shsmu.edu.cn

Full list of author information is available at the end of the article

the outer ring, while VD showed significant decreases in the nasal quadrants of the inner ring and the supratemporal and inferotemporal quadrant of the outer ring. Moreover, BMO-MRW was positively correlated with PD ($r=0.583$, $P=0.001$) and VD ($r=0.499$, $P=0.001$) in the inner ring, with positive correlations observed between BMO-MRW and inner PD and VD in the counterpart quadrants.

Conclusions Peripapillary BMO-MRW is significantly reduced in early DR, particularly in the superotemporal and inferotemporal quadrants, alongside declines in PD and VD. The positive correlation between BMO-MRW and microvascular parameters suggests its potential as a biomarker for early DR detection and monitoring.

Keywords Diabetic retinopathy, Optical coherence tomography angiography, Microvascular changes, BMO-MRW

Background

Diabetic retinopathy (DR), the leading cause of preventable vision loss in working-age populations [1], is traditionally classified as a microvascular disorder [2]. Emerging evidence indicates that retinal neurodegeneration precedes clinically detectable microvascular changes, manifesting as reduced contrast sensitivity, visual field defects, and electrophysiological abnormalities in diabetic patients [3, 4]. Preclinical studies in diabetic models and human donors reveal early neurodegenerative features—reactive gliosis, neuronal dysfunction, and apoptosis—prior to microaneurysm formation [5–7]. The neurovascular unit (NVU), a concept introduced by Rafael et al. [8], highlights the interdependence of neurons, glia, and micro-vessels in maintaining blood-retinal barrier integrity and regulating retinal perfusion [9]. Despite this, early DR lacks distinct clinical signs, and interventions remain largely reactive, targeting advanced stages with overt complications [10]. Improved understanding of early pathogenesis is critical for developing preventive strategies. Advances in optical coherence tomography (OCT) enable high-resolution retinal imaging, revealing subclinical neurodegeneration in diabetics without DR [11]. Thinning of the ganglion cell-inner plexiform layer (GC-IPL) and retinal nerve fiber layer (RNFL) precedes vascular damage, with accelerated RNFL thinning rates observed longitudinally [11–13]. Hyperglycemia disrupts NVU homeostasis via basement membrane thickening, pericyte loss, and neuroglial activation, exacerbating microcirculatory dysfunction [14]. Recent OCT innovations, such as Bruch's membrane opening-minimum rim width (BMO-MRW), demonstrate superior sensitivity to neurostructural damage compared to RNFL thickness (RNFLt) [12], though its utility in DR remains underexplored. Optical coherence tomography angiography (OCTA) studies confirm preclinical microvascular alterations in diabetics without DR, including reduced superficial/deep vessel density (VD) and perfusion density (PD) in paracentral, pericentral, and peripapillary regions [14–16]. However, existing OCTA protocols suffer from limitations: restricted scan areas (4.5 × 4.5 mm) [17, 18], crude quadrant-based analyses [19, 20], and failure to account for individual anatomical variability in the fovea-to-BMO (FoBMO) axis [21]. Standardized vertical/horizontal partitioning misaligns with patient-specific FoBMO angles (ranging 2.5° to -17.5°), compromising spatial accuracy [22].

This study employs FoBMO-axis calibrated OCTA to evaluate BMO-MRW and microvascular changes in early DR, investigating structural and vascular alterations concurrently.

Methods

This observational cross-sectional study was conducted in the Department of Ophthalmology at Shanghai Sixth People's Hospital from January 2021 to March 2025. This study conformed to the tenets of the Helsinki Declaration and was approved by the Ethics Committee of the Shanghai Sixth People's Hospital (No.2021-KY-091(K)). Informed consent was obtained from all the participants. Diabetic patients were recruited from Shanghai Sixth People's Hospital. Healthy controls were recruited from the medical examination center at the same hospital during the same period. For each diabetic patient, a detailed medical history, including diagnoses, medications, disease duration and laboratory tests, was recorded. We extracted the clinical data from recorded free text clinical notes and inpatient medical records. Inclusion criteria were (1) aged 18 years or older, (2) Whether T2DM was coupled with no DR or mild DR was evaluated by a retinal specialist through indirect fundoscopy and ultra widefield fundus photographs (Optomap Panoramic 200; Optos PLC). Mild DR was defined as microaneurysms only, according to the International Clinical Diabetic Retinopathy Disease Severity Scale.(3) had a refractive error within −3.00 diopters or +3 diopter-equivalent spheres. (4)BCVA ≤ 0.1logMAR; (5)22 mm< axial length<26 mm; (6) intraocular pressure<21mmHg. The exclusion criteria were as follows: (1) the presence of diabetic macular edema (DME); (2) having undergone previous intraocular surgery; (3) presenting with a disease affecting retinal function, including glaucoma, advanced cataracts or significant media opacity, or with other serious systemic disease.

All patients underwent comprehensive ophthalmic examination, including the ETDRS (Precision vision)

protocol visual acuity, slitlamp biomicroscopy, intraocular pressure measurement (TX-20 Canon, JAPAN) indirect stereoscopic fundus examination, and OCTA Spectralis HRA + OCT (Heidelberg Engineering, Germany).

Image acquisition and analysis

The radial scanning mode in the glaucoma module was selected, and 24 radial B-scan patterns were selected, with an angle of 7.5° between each B-scan line, and each image could also consist of 100 images superimposed on each other. A 6-mm × 6-mm macular scan was performed on both eyes of all participants using a Heidelberg OCTA Spectralis HRA + OCT (Heidelberg Engineering, Germany). The light source had a wavelength of 870 nm and contained 512 B-scans, with five consecutive scans for each B-scan of the same area. The participant's jaw was fixed in the jaw holder, and the refractive compensation was adjusted using the machine's refractive buttons through the internal fixation and kinesio-tracking modes of technology, and the images were acquired when the image was clear. A single 3D volumetric scan could acquire SLO, En-Face images, OCT images, and angiograms at the same time. All examinations are performed by the same physician(JZ). The scanning procedure was as follows: adjust the intracamera to the nasal side, select the OCTA mode, select a 6 × 6 mm rectangular scanning frame, and adjust the scanning frame to be centered on the optic papilla to perform the OCTA scan, which consists of 516 B-scans with an interval of 12 μm between each B-scan.

Peripapillary microvascular assessment was performed at the level of the superficial vascular complex (SVC). According to the parameter settings of the Heidelberg OCTA scanning equipment, the SVC layer was defined as 17 μm from the inner limiting membrane (ILM) to the IPL, and therefore the optic disc vascular density in this study included the radial peripapillary capillary (RPC), the superficial vascular plexus (SVP), and the peripapillary capillary (PPC). Images with obvious artifacts and signal intensity index < 20 were excluded, and only images with good imaging quality were included.

OCT angiography parameters

Image analysis was performed using FIJI, an open-source distribution of the program ImageJ. (i) Open the OCTA images in ImageJ, convert the OCTA images to 8-bit, and then analyze the OCTA images after the automatic "default" image analysis provided by the ImageJ software. The OCTA image is converted to 8-bit, automatically thresholded by the "default" threshold provided by the ImageJ software to neutralize the background noise, then converted to a binarized black-and-white image (Fig. 1A). This binarized image is used to calculate the Perfusion Density (PD): number of vascular pixels/total pixels in the analyzed area (%). (ii) A skeletonized image was then created from the binarized image, in which all vessels (including large vessels) were normalized to one pixel width, and all pixels in the skeleton image were measured and the vessel density (VD) was calculated as the number of vascular pixels × scanning width (mm)/area (mm^2) [17]. The region of interest (ROI) function of ImageJ software was used to partition the binarized and skeletonized optic disc OCTA images: first, the macula-optic disc axis (FoBMO axis) was marked on the original OCTA image and the FoBMO angle of the image was calculated, and then the rotational angle of the corresponding ROIs was set using this angle to perform ETDRS grid partitioning. ETDRS grid partitioning (three concentric circles with diameters of 1-, 3-, and 6-mm are used to divide the image into an inner ring between 1 and 3 mm and an outer ring between 3 and 6 mm. The inner and outer rings were divided into six quadrants of Superonasal, supratemporal, lateral temporal, Inferotemporal, Inferonasal, and lateral nasal, with a total of twelve regions using ROIs adjusted according to the FoBMO-axis (Fig. 1B), and the PD and VD values of the inner and outer rings as well as those of each region were acquired separately(Fig. 1C and D). All images were saved and analyzed anonymously.

Statistical analysis

Baseline data of the three groups of subjects were compared and quantitative variables were expressed as (mean ± standard deviation). Qualitative variables were expressed as number, for the included studies data were analyzed by Kolmogorov-Smirnov test for obeying normal distribution, one-way ANOVA was used for continuous normally distributed variables, and differences between groups were performed using Bonferroni post hoc test. Independent samples t-test Mann-Whitney U test was performed to compare continuous variables. Categorical variables were tested using chi-square test.

Correlation between variables was assessed using Pearson correlation test. All analyses were performed using the statistical version of the software SPSS 26.0 (IBM Corporation, Chicago, IL, USA) and differences were considered statistically significant at $P < 0.05$.

Results

The study included 105 eyes from 105 diabetic patients, comprising 55 eyes without diabetic retinopathy (No-DR group) and 50 eyes with mild diabetic retinopathy (Mild-DR group), and 50 healthy eyes from 50 participants of the control group. The baseline information is shown in Table 1. There was no statistically significant difference in age, gender, laterality, spherical equivalent, intraocular pressure, FoBMO angle and axial length between

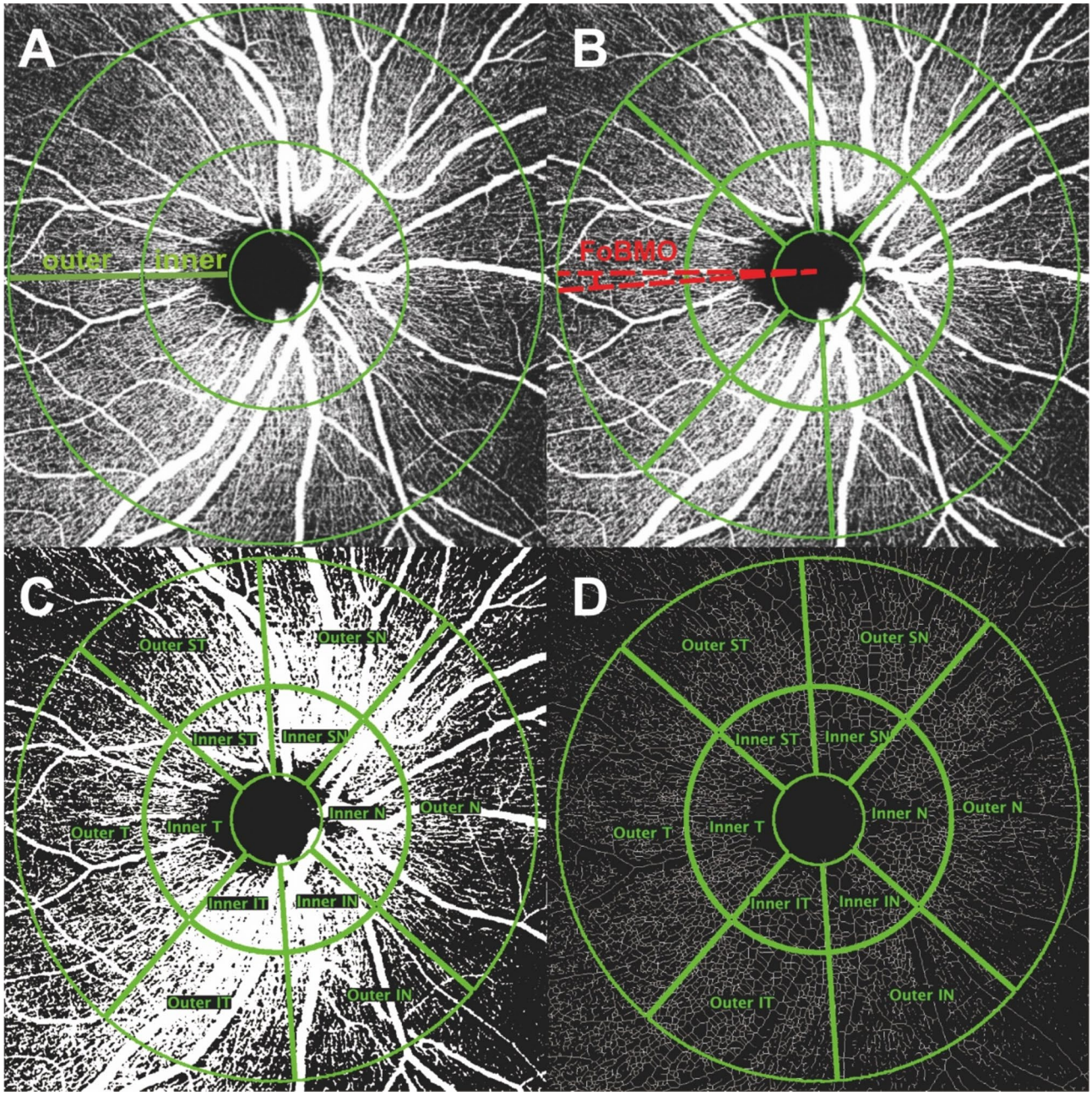

Fig. 1 Image processing and measurement of PD and VD. **A**, Original grayscale OCT angiography image of peripapillary vascular. **B**, a total of twelve regions using ROIs adjusted according to the specific FoBMO angle. **C**, calculated twelve regions of perfusion density after binarized. **D**, calculated twelve regions of vessel density after skeletonized

the three groups. The BCVA of control group was significantly better than No-DR group and Mild-DR group ($P = 0.004$), and the difference in the duration of diabetes mellitus and glycosylated hemoglobin (HbA1c) between the two groups of diabetic patients was not statistically significant ($P = 0.825$, 0.077, respectively).

BMO-MRW

The average BMO-MRW and values for the ETDRS quadrants in the control, No-DR, and Mild-DR groups are presented in Table 2. The average BMO-MRW were (323.56 ± 40.33) μm, (305.78 ± 35.12) μm, and (299.42 ± 37.33) μm for the control, No-DR, and Mild-DR groups, respectively ($P = 0.005$). Both the No-DR and Mild-DR groups had significantly lower BMO-MRW compared to the control group ($P = 0.017$,

Table 1 Demographic and clinical characteristic of three groups

	Control group($n=50$)	No-DR group ($n=55$)	Mild-DR group($n=50$)	*P*-value
Age (mean ± SD), yrs	56.10 ± 8.57	57.60 ± 8.02	54.42 ± 10.29	0.197
Gender (male/female)	24/26	30/25	25/25	0.787△
Laterality (right/left)	28/22	31/24	26/24	0.886△
BCVA(logMAR)	-0.01 ± 0.07	0.00 ± 0.06	0.04 ± 0.09	0.004*
Spherical equivalent (D)	0.24 ± 0.92	-0.15 ± 1.19	-0.13 ± 1.20	0.144
IOP (mmHg)	15.05 ± 2.59	15.18 ± 2.41	15.33 ± 3.00	0.873
FoBMO angle (°)	-7.72 ± 3.55	-6.78 ± 3.67	-7.04 ± 3.33	0.382
Axial length (mm)	23.21 ± 0.56	23.45 ± 0.73	23.27 ± 0.77	0.178
Duration of diabetes (y)	NA	11.00 ± 7.33	10.38 ± 6.93	0.825#
HbA1c (mean ± SD), %	NA	7.60 ± 1.54	8.20 ± 1.77	0.077#

△ chi-square test; # T-test; * $P<0.05$

BCVA, best corrected visual acuity; IOP, Intraocular pressure; HbA1c, glycated hemoglobulin; NA, not applicable; No-DR, patients with diabetes without clinically detectable retinopathy; Mild-DR, patients with diabetes only with microaneurysms

Table 2 Comparison of the BMO-MRW among three groups

	Control group($n=50$)	No-DR group ($n=55$)	Mild-DR group($n=50$)	*P*	P_1	P_2	P_3
BMO-MRW (μm)							
Average	323.56 ± 40.33	305.78 ± 35.12	299.42 ± 37.33	**0.005***	**0.017***	**0.002***	0.388
Superonasal	361.62 ± 46.22	359.73 ± 49.07	354.70 ± 59.30	0.787			
Nasal	336.94 ± 55.50	314.87 ± 70.00	318.18 ± 52.42	0.133			
Inferonasal	383.68 ± 45.19	364.22 ± 55.53	363.76 ± 57.84	0.102			
Inferotemporal	357.18 ± 60.07	336.62 ± 44.94	332.68 ± 53.39	**0.047***	**0.049***	**0.022***	0.704
Temporal	242.74 ± 55.14	221.82 ± 39.51	223.42 ± 50.42	0.056			
Superotemporal	325.16 ± 43.30	308.35 ± 39.72	304.52 ± 45.33	**0.039***	**0.046***	**0.017***	0.648

BMO-MRW: Bruch's Membrane Opening-Minimum Rim Width; No-DR, patients with diabetes without clinically detectable retinopathy; Mild-DR, patients with diabetes only with microaneurysms

One-way ANOVA: P, one-way analysis of variance followed by post-hoc Bonferroni test; P1,control vs. No-DR group; P2,control vs. Mild-DR group; P3,No-DR group vs. Mild-DR group

*$P<0.05$ is considered as statically significant

0.002, respectively), though no significant difference was observed between the No-DR and Mild-DR groups ($P=0.388$). In the ETDRS quadrants, significant decreases in BMO-MRW were observed between the three groups, particularly in the supratemporal and inferotemporal quadrants. In the supratemporal quadrant, BMO-MRW decreased from (325.16 ± 43.30) μm in the control group to (308.35 ± 39.72) μm in the No-DR group, reaching the lowest value of (304.52 ± 45.33) μm in the Mild-DR group ($P=0.046$, 0.017), with no significant difference between the No-DR and Mild-DR groups ($P=0.648$). In the inferotemporal quadrant, the BMO-MRW values were (357.18 ± 60.07) μm, (336.62 ± 44.94) μm, and (332.68 ± 53.39) μm for the control, No-DR, and Mild-DR groups, respectively ($P=0.047$). Both the No-DR and Mild-DR groups were significantly lower than the control group ($P=0.049$, 0.002), but no significant difference was found between the No-DR and Mild-DR groups ($P=0.489$). No statistically significant differences in BMO-MRW were found between the three groups in the superonasal, lateral nasal, inferonasal, and temporal quadrants.

Peripapillary perfusion density (PD)

The distribution of peripapillary vascular perfusion density (PD) in the optic disc for the control, No-DR, and Mild-DR groups is presented in Table 3. The average PD in the inner ring was (56.01 ± 10.53)%, (52.16 ± 8.75)%, and (47.91 ± 12.95)% for the control, No-DR, and Mild-DR groups, respectively ($P=0.001$). The Mild-DR group exhibited significantly lower PD compared to the control group ($P<0.001$) and the No-DR group ($P=0.046$), with no significant difference observed between the No-DR and control groups ($P=0.071$). In the inner ring of the ETDRS grid, significant differences were found in the nasal quadrant ($P<0.001$), although no significant differences were observed in other quadrants. For the outer ring of the ETDRS grid, the average PD values were (42.92 ± 6.70)%, (40.20 ± 7.24)%, and (38.13 ± 8.78)% for the three groups, respectively ($P=0.008$). The Mild-DR group showed significantly lower PD compared to the control group ($P=0.002$), but no significant difference was found between the Mild-DR and No-DR groups ($P=0.069$) or between the Mild-DR and control groups ($P=0.168$). The only significant difference in

Table 3 Comparison of peripapillary perfusion density and vessel density among three groups

	Control group ($n=50$)	No-DR group ($n=55$)	Mild-DR group ($n=50$)	*P*-value			
				P	P_1	P_2	P_3
Perfusion Density (PD)							
1–3 mm inner (%)							
Average	56.01 ± 10.53	52.16 ± 8.75	47.91 ± 12.95	**0.001***	0.071	**<0.001***	**0.046***
Superonasal	60.51 ± 16.09	57.24 ± 15.37	54.46 ± 17.27	0.179			
Nasal	53.71 ± 13.55	44.58 ± 13.22	37.90 ± 15.48	**<0.001***	**0.001***	**<0.001***	**0.017***
Inferonasal	68.38 ± 14.78	65.21 ± 12.36	62.87 ± 16.25	0.166			
Inferotemporal	72.57 ± 14.03	70.46 ± 13.18	65.84 ± 17.08	0.070			
Temporal	40.37 ± 12.87	37.16 ± 12.41	36.38 ± 12.87	0.251			
Superotemporal	54.25 ± 15.60	55.05 ± 15.85	50.50 ± 16.38	0.306			
3–6 mm outer (%)							
Average	42.92 ± 6.70	40.20 ± 7.24	38.13 ± 8.78	**0.008***	0.069	**0.002***	0.168
Superonasal	47.40 ± 13.01	44.07 ± 13.00	41.35 ± 15.50	0.112			
Nasal	29.27 ± 7.92	27.08 ± 10.69	25.04 ± 9.66	0.090			
Inferonasal	36.52 ± 12.82	35.87 ± 12.90	37.57 ± 13.24	0.799			
Inferotemporal	71.03 ± 10.57	65.47 ± 13.16	65.58 ± 17.22	0.073			
Temporal	38.52 ± 10.58	36.04 ± 12.16	35.35 ± 9.69	0.312			
Superotemporal	60.96 ± 11.95	57.91 ± 12.03	53.19 ± 17.96	**0.024***	0.272	**0.007***	0.091
Vessel density(VD)							
Inner 1–3 mm (mm^{-1})							
Average	15.41 ± 2.68	14.39 ± 2.17	13.55 ± 2.98	**0.002***	**0.048**	**<0.001***	0.102
Superonasal	13.69 ± 3.30	13.38 ± 3.42	12.61 ± 3.58	0.268			
Nasal	15.71 ± 3.72	13.00 ± 3.48	11.19 ± 4.36	**<0.001***	**<0.001***	**<0.001***	**0.018***
Inferonasal	15.76 ± 3.17	15.13 ± 2.49	14.37 ± 3.84	0.096			
Inferotemporal	16.05 ± 3.09	15.53 ± 3.08	15.03 ± 2.57	0.225			
Temporal	15.69 ± 4.22	14.34 ± 4.15	13.74 ± 4.73	0.076			
Superotemporal	15.65 ± 3.95	15.14 ± 3.44	14.45 ± 3.61	0.262			
Outer 3–6 mm (mm^{-1})							
Average	13.74 ± 2.26	12.78 ± 2.53	12.09 ± 2.83	**0.006***	0.057	**0.002***	0.157
Superonasal	13.40 ± 3.69	12.46 ± 3.79	12.99 ± 3.67	0.665			
Nasal	10.61 ± 3.04	9.62 ± 4.26	9.28 ± 3.71	0.181			
Inferonasal	11.07 ± 4.12	10.44 ± 3.91	10.89 ± 4.13	0.712			
Inferotemporal	18.02 ± 2.56	16.60 ± 3.09	16.23 ± 4.44	**0.025***	**0.036***	**0.010***	0.585
Temporal	15.45 ± 3.87	14.49 ± 4.48	13.93 ± 4.85	0.223			
Superotemporal	17.84 ± 2.92	16.53 ± 3.31	15.67 ± 6.09	**0.044***	0.122	**0.013***	0.314

No-DR, patients with diabetes without clinically detectable retinopathy; Mild-DR, patients with diabetes only with microaneurysms

One-way ANOVA: P, one-way analysis of variance followed by post-hoc Bonferroni test; P1,control vs. No-DR group; P2,control vs. Mild-DR group; P3,No-DR group vs. Mild-DR group

*$P<0.05$ is considered as statically significant

the outer ring was found in the superotemporal quadrant ($P=0.024$), where the PD values in the Mild-DR group were significantly lower than those in the control group ($P=0.007$). No significant difference was observed between the Mild-DR group and No-DR or between the Mild-DR and control groups ($P=0.272$, 0.091).

Peripapillary vascular density (VD)

The distribution of peripapillary vascular density (VD) in the optic disc across the control, No-DR, and Mild-DR groups was also presented in Table 3. The average VD in the inner ring was (15.51 ± 2.66) mm^{-1}, (14.52 ± 2.20) mm^{-1}, and (12.89 ± 2.97) mm^{-1} for the control, No-DR, and Mild-DR groups, respectively ($P=0.002$). The Mild-DR group showed a significantly lower VD than the control group ($P<0.001$), but no significant difference was found between the Mild-DR and No-DR groups ($P=0.052$) or between the Mild-DR and control groups ($P=0.102$). In the outer ring, a significant difference in VD was observed only in the nasal quadrant among the three groups ($P<0.001$). The average VD values in the outer ring were (13.74 ± 2.26) mm^{-1}, (12.78 ± 2.53) mm^{-1}, and (12.09 ± 2.83) mm^{-1} for the control, No-DR, and Mild-DR groups, respectively ($P=0.006$). Significant differences in VD in the outer ring of the ETDRS grid were found in the inferotemporal and superotemporal

Table 4 Correlation analyses between BMO-MRW and perfusion density/vessel density (average and six quadrant)

		BMO-MRW						
		Average	**SN**	***N***	**IN**	**IT**	**T**	**ST**
PD								
	Inner Average	**0.583***	**0.419***	**0.518***	**0.448***	**0.273***	**0.455***	**0.470***
	Outer Average	0.052	0.028	0.088	0.014	-0.107	0.118	0.074
	Inner SN	0.427*	**0.407***	0.335*	0.384*	0.262*	0.288*	0.341*
	Outer SN	-0.055	0.045	-0.028	-0.003	-0.131	-0.053	-0.051
	Inner N	0.516*	0.357*	**0.564***	0.495*	0.178*	0.363*	0.374*
	Outer N	-0.143	-0.133	-0.015	-0.103	-0.202*	-0.036	-0.118
	Inner IN	0.589*	0.427*	0.545*	**0.548***	0.210*	0.414*	0.369*
	Outer IN	0.014	-0.011	0.128	0.011	-0.176	0.067	-0.049
	Inner IT	0.515*	0.401*	0.417*	0.433*	**0.381***	0.330*	0.358*
	Outer IT	0.202*	0.117	0.218	0.189	-0.036	0.171	0.126
	Inner T	0.319*	0.163*	0.241*	0.102	0.141	**0.368***	0.350*
	Outer T	0.130	0.026	0.065	0.002	-0.017	0.169	0.180
	Inner ST	0.358*	0.265*	0.222*	0.133	0.207*	0.350*	**0.411***
	Outer ST	0.118	0.064	-0.003	0.048	0.106	0.183	**0.202***
VD								
	Inner Average	**0.499***	**0.355***	**0.433***	**0.348***	**0.215***	**0.405***	**0.448***
	Outer Average	0.048	0.007	0.086	-0.007	-0.136	0.128	0.082
	Inner SN	0.383*	**0.295***	0.271*	0.288*	0.165*	0.309*	0.361*
	Outer SN	-0.006	0.040	-0.025	-0.012	-0.039	0.008	0.071
	Inner N	0.449*	0.285*	**0.456***	0.390*	0.158*	0.331*	0.334*
	Outer N	-0.121	-0.131	0.006	-0.123	-0.235*	-0.015	-0.061
	Inner IN	0.339*	0.232*	0.303*	**0.299***	0.140	0.268*	0.220*
	Outer IN	0.021	-0.033	0.141	0.021	-0.194	0.083	-0.053
	Inner IT	0.308*	0.289*	0.258*	0.286*	**0.245***	0.130	0.207*
	Outer IT	0.106	0.108	0.119	0.144	0.015	0.061	0.041
	Inner T	0.273*	0.165*	0.228*	0.090	0.104	**0.301***	0.320*
	Outer T	0.123	0.065	0.092	0.004	-0.010	0.146	0.165*
	Inner ST	0.337*	0.299*	0.254*	0.178*	0.199*	0.294*	**0.353***
	Outer ST	0.167*	0.114	0.038	0.079	0.088	0.198*	**0.233***

BMO-MRW, Bruch's Membrane Opening-Minimum Rim Width; PD, perfusion density; VD, vessel density; Inner, inner ring of ETDRS grid; Outer, outer ring of ETDRS grid;

SN, superonasal; N, nasal; IN, inferonasal; IT, inferotemporal; T, temporal; ST, superotemporal

* The correlation calculated by Pearson test showed $P<0.05$

quadrants ($P=0.025$, 0.044), with VD in the Mild-DR group significantly lower than in the control group ($P=0.010$, 0.013). In the inferotemporal quadrant, a significant difference was observed between the control and No-DR groups ($P=0.025$), although no significant difference was found between the Mild-DR and control groups. In the superotemporal quadrant, no significant difference was observed between the Mild-DR and No-DR groups or the control group ($P=0.314$, 0.122).

Correlation analysis of BMO-MRW and perfusion density/vessel density

Table 4 shows correlations between BMO-MRW values (average and separately in each quadrant) and PD/VD. The average PD in the inner ring was positively correlated with the average BMO-MRW($r=0.583$, $P=0.001$). Superonasal, nasal, Inferonasal, inferotemporal, temporal, and supratemporal quadrant inner ring PDs were all positively correlated with the BMO-MRW of the corresponding quadrants. PDs were positively correlated with the BMO-MRW of the outer ring of the supratemporal quadrant ($r=0.202$, $P=0.013$). The average VD in the inner ring was positively correlated with the average BMO-MRW($r=0.499$, $P=0.001$). The Superonasal, nasal, Inferonasal, inferotemporal, temporal, and supratemporal quadrant inner ring VD were all positively correlated with the BMO-MRW of the corresponding quadrants, VD were positively correlated with the BMO-MRW of the outer ring of the supratemporal quadrant ($r=0.233$, $P=0.004$).

Discussion

This study employed Heidelberg OCTA to evaluate changes in BMO-MRW and the superficial capillary layer of the peripapillary retina in healthy individuals, patients without diabetic retinopathy (No-DR), and those with early diabetic retinopathy (Mild-DR). Our study focused on the peripapillary optic disc region and used BMO-MRW, a more sensitive indicator than RNFLt, to assess nerve fiber changes and analyze the relationship between optic nerve thickness and microvascular alterations [23, 24]. Our findings indicate that, compared to healthy individuals, diabetic patients exhibited a significant reduction in BMO-MRW, with this decrease already evident in the No-DR group. Using the ETDRS grid, we further analyzed BMO-MRW of the optic disc in six quadrants. In both the No-DR and Mild-DR groups, BMO-MRW in the superior temporal and inferior temporal quadrants was significantly thinner than in the control group. Additionally, all data were partitioned based on the FoBMO axis, as the FoBMO angle varies significantly between individuals and is highly susceptible to examination posture, potentially affecting DR progression assessment. Compared to previous methods, our approach aligns more closely with anatomical structures and may more accurately reflect the true pathophysiological changes in diabetic patients [25, 26].

Sabry et al. [27] also investigated BMO-MRW changes in patients without diabetic retinopathy. Their results showed no significant difference in the mean BMO-MRW between healthy controls and diabetic patients. In the supratemporal quadrant, BMO-MRW decreased from (342.94 ± 52.19) μm in the No-DR group to (323.60 ± 52.42) μm in the healthy control group, while in the inferotemporal quadrant, it decreased from (362.84 ± 60.24) μm to (356.92 ± 60.24) μm. However, no significant difference was found between the two groups. Considering that this study included only 19 cases (38 eyes) in both the control and No-DR groups, the small sample size may have influenced the results.

Vascular analysis of the optic disc showed that in both the inner and outer rings, vessel density in the superior and inferior temporal quadrants was higher than in other quadrants, indicating a relatively richer blood supply in these regions. Anatomically, nerve fibers from the macula and peripheral retina converge in an arc toward the optic disc along the superior and inferior sides of the macula-optic disc axis. Consequently, the superior temporal and inferior temporal regions of the optic disc exhibit denser vasculature than other areas [27]. Additionally, the superficial capillary layer of the optic disc, particularly the radial peripapillary capillaries (RPC), runs parallel to the nerve axons, forming relatively straight vessels with limited anastomoses, making them less tolerant to hypoxia and damage [28]. This anatomical arrangement renders them more susceptible to hypoxic injury. The high neural density in the superotemporal and inferotemporal quadrants further contributes to an increased oxygen demand, potentially exacerbating their vulnerability to structural alterations under hyperglycemic conditions, as reflected by the observed BMO-MRW thinning. Notably, this change was not observed in PD in the inner ring of the superotemporal and inferotemporal quadrants, whereas vessel density (VD) alterations were detected in the outer ring. As a skeletonized image, VD standardizes the influence of both large and small vessels, reducing the effect of vessel diameter on retinal perfusion measurements. This makes VD theoretically more accurate than PD in assessing vascular changes [29, 30].

Most previous studies have focused on the macular region in DR patients, identifying structural changes across different retinal layers [7, 31, 32]. Some have also explored microvascular changes around the optic disc in diabetic patients, demonstrating a significant correlation between RPC vessel density and retinal nerve fiber layer thickness (RNFLt) [33–35]. In an OCTA-based study, Cao et al. compared optic disc vessel density and RNFLt in normal individuals and hyperglycemic patients without diabetic retinopathy [36]. They found that all quadrants of the No-DR group exhibited significant vessel density changes, whereas RNFLt showed significant changes only in the superior nasal, inferior nasal, and nasal quadrants—differing from the BMO-MRW changes observed in our study. These discrepancies may stem from differences in imaging equipment, observation area size, and partitioning methods. In our study, changes were detected in the superior temporal and inferior temporal quadrants, whereas in their study, these regions were partly classified under the inferior nasal and superior nasal quadrants. This underscores the importance of considering partitioning methods when comparing results across studies and highlights the need for standardized optic disc segmentation.

Additionally, our study found that in No-DR patients, PD and VD changes in the nasal and inferonasal quadrants of the inner ring occurred earlier than BMO-MRW changes. This aligns with previous findings indicating thinning in these regions, suggesting that nasal quadrant blood flow alterations warrant further investigation. Earlier research using RNFL to study diabetic patients divided the optic disc region into superior, nasal, inferior, and temporal quadrants, identifying early RNFL thinning in the inferior quadrant of diabetic patients without DR. Our study used BMO-MRW, a more sensitive parameter than RNFLt, and similarly found that BMO-MRW in the superior temporal and inferior temporal quadrants was already significantly thinner in diabetic patients without DR compared to healthy individuals. However, in these groups, PD and VD changes around the optic disc were

not statistically significant compared to normal individuals. This suggests that BMO-MRW may serve as a valuable biomarker for distinguishing and monitoring diabetic retinopathy progression in diabetic patients.

We further investigated the correlation between BMO-MRW and PD/VD around the optic disc and found a positive correlation in the corresponding quadrants of the standardized ETDRS inner ring. This may be because the inner ring is anatomically closer to the BMO-MRW, leading to a stronger correlation. The observed thinning of neural tissue and decreased vascular density in early DR suggest a potential relationship between neural tissue integrity and vascular density, reinforcing the concept of the "optic nerve vascular unit." Diabetic patients without fundus lesions exhibit lower VD and PD in the optic disc region than healthy individuals, indicating that optic disc vascular density could serve as an indicator of microvascular changes in diabetes.

There are still several limitations in this study. First, as a cross-sectional observational study, it cannot establish a causal relationship between neurodegenerative changes and microvascular alterations in the optic disc region of diabetic patients. Future prospective longitudinal studies are necessary to clarify this temporal relationship. Second, our vascular density measurement method differs from previous studies; we used a 6 mm × 6 mm blood flow density assessment of the optic disc region, simultaneously observing the superficial capillaries, radial peripapillary capillary layer, and macrovascular structures. Currently, no ideal method exists to evaluate the peripapillary capillary layer separately. Future advancements in ophthalmic imaging technology may enable the development of techniques and algorithms capable of distinguishing capillary and macrovascular layers. Furthermore, based on the observed neural and vascular structural changes in DR patients, a feasible preclinical grading system for DR could be established. Through close follow-up and precise interventions, we may delay or even prevent DR progression, ultimately protecting more patients from severe vision loss and irreversible retinal damage.

Conclusions

This study demonstrates that peripapillary BMO-MRW is significantly reduced in early diabetic retinopathy, particularly in the superotemporal and inferotemporal quadrants. Concurrent declines in peripapillary perfusion density and vessel density were observed, notably in the nasal, superotemporal, and inferotemporal quadrants. The positive correlation between BMO-MRW and both PD and VD suggests a strong association between neuroretinal rim thinning and microvascular changes in early DR. These findings underscore the potential of BMO-MRW and OCTA-derived microvascular metrics as early biomarkers for DR detection and progression monitoring.

Acknowledgements
The authors thanks to Dr. Yuchen Zhao for his great supports for data analysis of this work.

Author contributions
XYZ, QW had full access to all data in the study and takes responsibility for the integrity of the data and the accuracy of the data analysis. Study concept and design: JZ, XNW, WL. Acquisitions, analysis, or interpretation of data: JZ, XNW, TTL, YZ. Drafting of the manuscript: ZJ, XNW, WL. Critical revision of the manuscript for important intellectual content: XYZ, QW.Statistical Analysis: JZ, YH, DL, Administrative, technical, or material support: TTL, YZ. All authors read and approved the final manuscript.

Funding
This work was Supported by the College-level Project Fund of Shanghai Sixth People's Hospital (Grant No. ynlc201909) and the Interdisciplinary Program of Shanghai Jiao tong University (Project No. YG2022QN089).

Data availability
The datasets used and/or analysed during the current study available from the corresponding author on reasonable request.

Declarations

Ethics approval and consent to participate
The study adhered to the guidelines of the Helsinki Declaration and had the approval of the Ethics Committee of Sixth People's Hospital Affiliated to Shanghai Jiao Tong University, Shanghai, China. (No.2021-KY-091(K)). All patients signed written informed consent for participation.

Consent for publication
Not applicable.

Competing interests
The authors declare no competing interests.

Author details
[1]Department of Ophthalmology, Shanghai Sixth People's Hospital Affiliated to Shanghai Jiao Tong University School of Medicine, Shanghai Jiao Tong University, Shanghai 200233, P.R. China

Received: 29 March 2024 / Accepted: 16 April 2025
Published online: 28 April 2025

References

1. Cheung N, Mitchell P, Wong TY. Diabetic retinopathy. Lancet. 2010;376:13.
2. Simó R, Hernández C, European Consortium for the Early Treatment of Diabetic Retinopathy (EUROCONDOR). Neurodegeneration in the diabetic eye: new insights and therapeutic perspectives. Trends Endocrinol Metab. 2014;25:23–33.
3. Barber AJ, Baccouche B. Neurodegeneration in diabetic retinopathy: potential for novel therapies. Vis Res. 2017;139:82–92.
4. Simó R, Hernández C. Novel approaches for treating diabetic retinopathy based on recent pathogenic evidence. Prog Retin Eye Res. 2015;48:160–80.
5. Abcouwer SF, Gardner TW. Diabetic retinopathy: loss of neuroretinal adaptation to the diabetic metabolic environment. Ann N Y Acad Sci. 2014;1311:174–90.
6. Barber AJ, Lieth E, Khin SA, Antonetti DA, Buchanan AG, Gardner TW. Neural apoptosis in the retina during experimental and human diabetes. Early onset and effect of insulin. J Clin Invest. 1998;102:783–91.
7. Wang X, Cai X, Li S, Li T, Long D, Wu Q, et al. Wide-field swept-source OCTA in the assessment of retinal microvasculature in early-stage diabetic retinopathy. BMC Ophthalmol. 2022;22:473.
8. Simó R, Stitt AW, Gardner TW. Neurodegeneration in diabetic retinopathy: does it really matter? Diabetologia. 2018;61:1902–12.

9. Staurenghi G, Sadda S, Chakravarthy U, Spaide RF. International nomenclature for optical coherence tomography (IN•OCT) panel. Proposed lexicon for anatomic landmarks in normal posterior segment spectral-domain optical coherence tomography: the IN•OCT consensus. Ophthalmology. 2014;121:1572–8.
10. Chakravarthy H, Devanathan V, Chakravarthy H, Devanathan V. Molecular mechanisms mediating diabetic retinal neurodegeneration: potential research avenues and therapeutic targets. J Mol Neurosci. 2018;66:445–61.
11. Ishikawa H, Stein DM, Wollstein G, Beaton S, Fujimoto JG, Schuman JS. Macular segmentation with optical coherence tomography. Invest Ophthalmol Vis Sci. 2005;46:2012–7.
12. Lim HB, Shin YI, Lee MW, Park GS, Kim JY. Longitudinal changes in the peripapillary retinal nerve fiber layer thickness of patients with type 2 diabetes. JAMA Ophthalmol. 2019;137:1125–32.
13. Li S-T, Wang X-N, Du X-H, Wu Q. Comparison of spectral-domain optical coherence tomography for intra-retinal layers thickness measurements between healthy and diabetic eyes among Chinese adults. PLoS ONE. 2017;12:e0177515.
14. Roy S, Kim D, Roy S, Kim D. Retinal capillary basement membrane thickening: role in the pathogenesis of diabetic retinopathy. Prog Retin Eye Res. 2021;82:100903.
15. Das A, McGuire PG, Rangasamy S. Diabetic macular edema: pathophysiology and novel therapeutic targets. Ophthalmology. 2015;122:1375–94.
16. Dimitrova G, Chihara E, Takahashi H, Amano H, Okazaki K. Quantitative retinal optical coherence tomography angiography in patients with diabetes without diabetic retinopathy. Investig Ophthalmol Vis Sci. 2017;58:190–6.
17. Shin Y-I, Nam KY, Lee SE, Lee M-W, Lim H-B, Jo Y-J, et al. Peripapillary microvasculature in patients with diabetes mellitus: an optical coherence tomography angiography study. Sci Rep. 2019;9:15814.
18. Vujosevic S, Muraca A, Gatti V, Masoero L, Brambilla M, Cannillo B, et al. Peripapillary microvascular and neural changes in diabetes mellitus: an OCT-Angiography study. Invest Ophthalmol Vis Sci. 2018;59:5074.
19. Zeng Y, Cao D, Yu H, Yang D, Zhuang X, Hu Y, et al. Early retinal neurovascular impairment in patients with diabetes without clinically detectable retinopathy. Br J Ophthalmol. 2019;103:1747–52.
20. Frizziero L, Parrozzani R, Londei D, Pilotto E, Midena E, Frizziero L, et al. Quantification of vascular and neuronal changes in the peripapillary retinal area secondary to diabetic retinopathy. Br J Ophthalmol. 2021;105:1577–83.
21. Chauhan BC, Burgoyne CF. From clinical examination of the optic disc to clinical assessment of the optic nerve head: a paradigm change. Am J Ophthalmol. 2013;156:218–e2272.
22. Chauhan BC, Danthurebandara VM, Sharpe GP, Demirel S, Girkin CA, Mardin CY, et al. Bruch's membrane opening minimum rim width and retinal nerve fiber layer thickness in a normal white population. Ophthalmology. 2015;122:1786–94.
23. Cho H-K, Kee C. Rate of change in Bruch's membrane opening-minimum rim width and peripapillary RNFL in early normal tension glaucoma. J Clin Med. 2020;9:E2321.
24. Gmeiner JMD, Schrems WA, Mardin CY, Laemmer R, Kruse FE, Schrems-Hoesl LM. Comparison of Bruch's membrane opening minimum rim width and peripapillary retinal nerve fiber layer thickness in early glaucoma assessment. Invest Ophthalmol Vis Sci. 2016;57:OCT575–584.
25. Pekel E, Tufaner G, Kaya H, Kaşıkçı A, Deda G, Pekel G. Assessment of optic disc and ganglion cell layer in diabetes mellitus type 2. Med (Baltim). 2017;96:e7556.
26. Jia Y, Simonett JM, Wang J, Hua X, Liu L, Hwang TS, et al. Wide-Field OCT angiography investigation of the relationship between radial peripapillary capillary plexus density and nerve Fiber layer thickness. Invest Ophthalmol Vis Sci. 2017;58:5188–94.
27. Yu PK, Balaratnasingam C, Xu J, Morgan WH, Mammo Z, Han S, et al. Label-Free density measurements of radial peripapillary capillaries in the human retina. PLoS ONE. 2015;10:e0135151.
28. Campbell JP, Zhang M, Hwang TS, Bailey ST, Wilson DJ, Jia Y, et al. Detailed vascular anatomy of the human retina by Projection-Resolved optical coherence tomography angiography. Sci Rep. 2017;7:42201.
29. Ghasemi Falavarjani K, Al-Sheikh M, Darvizeh F, Sadun AA, Sadda SR, Ghasemi Falavarjani K, et al. Retinal vessel calibre measurements by optical coherence tomography angiography. Br J Ophthalmol. 2017;101:989–92.
30. Kim AY, Chu Z, Shahidzadeh A, Wang RK, Puliafito CA, Kashani AH. Quantifying microvascular density and morphology in diabetic retinopathy using Spectral-Domain optical coherence tomography angiography. Invest Opthalmology Visual Sci. 2016;57:362–70.
31. Kim T-Y, Song Y-Y, Il-Jung, Na Y-J, Lee Y-H, Kim J-Y, et al. The impairment of the deep vascular complex in prolonged type 2 diabetes patients without clinical diabetic retinopathy. PLoS ONE. 2022;17:e0269182.
32. Aschauer J, Pollreisz A, Karst S, Hülsmann M, Hajdu D, Datlinger F, et al. Longitudinal analysis of microvascular perfusion and neurodegenerative changes in early type 2 diabetic retinal disease. Br J Ophthalmol. 2022;106:528–33.
33. Lee M-W, Lee J-W, Lee K-H, Lee Y-H, Kim J-Y. Peripapillary RNFL/vessel density ratio in patients with type2 diabetes without clinical diabetic retinopathy. Sci Rep. 2022;12:9463.
34. Zhang M, Jia F, Li N, Song C, Yang J, Yang K, et al. Quantitative analysis of the RPC vessel density and the RNFL thickness in patients with type 2 diabetes mellitus by using OCT angiography. Ophthalmic Res. 2021;64:951–9.
35. Yang HS, Woo JE, Kim M-H, Kim DY, Yoon YH. Co-Evaluation of peripapillary RNFL thickness and retinal thickness in patients with diabetic macular edema: RNFL misinterpretation and its adjustment. PLoS ONE. 2017;12:e0170341.
36. Cao D, Yang D, Yu H, Xie J, Zeng Y, Wang J, et al. Optic nerve head perfusion changes preceding peripapillary retinal nerve fibre layer thinning in preclinical diabetic retinopathy. Clin Exp Ophthalmol. 2019;47:219–25.

Publisher's note